# ATR-FTIR Spectroscopy and Isotope Labeling of the $P_M$ Intermediate of *Paracoccus denitrificans* Cytochrome *c* Oxidase†

Masayo Iwaki,‡ Anne Puustinen,§ Mårten Wikström,§ and Peter R. Rich*,‡

*Glynn Laboratory of Bioenergetics, Department of Biology, University College London, Gower Street, London WC1E 6BT, U.K., and Helsinki Bioenergetics Group, Programme for Structural Biology and Biophysics, Institute of Biotechnology, University of Helsinki, PB 65 (Viikinkaari 1), University of Helsinki, FI-00014 Helsinki, Finland*

*Received July 9, 2004; Revised Manuscript Received September 9, 2004*

ABSTRACT: The structure of the $P_M$ intermediate of *Paracoccus denitrificans* cytochrome *c* oxidase was investigated by perfusion-induced attenuated total reflection-Fourier transform infrared (ATR-FTIR) spectroscopy. Transitions from the oxidized to $P_M$ state were initiated by perfusion with CO/oxygen buffer, and the extent of conversion was quantitated by simultaneously monitoring visible absorption changes. In prior work, tentative assignments of bands were proposed for heme $a_3$, a change in the environment of the protonated state of a carboxylic acid, and a covalently linked histidine−tyrosine ligand to $Cu_B$ that has been found in the catalytic site. In this work, reduced minus oxidized difference spectra at pH 6.5 and 9.0 and $P_M$ minus oxidized difference spectra at pH 9.0 were compared in unlabeled, universally $^{15}N$-labeled, and tyrosine-ring-$d_4$-labeled proteins to improve these assignments. In the reduced minus oxidized difference spectrum, $^{15}N$ labeling resulted in large changes in the amide II region and a 9 $cm^{-1}$ downshift in a 1105 $cm^{-1}$ trough that is attributed to histidine. In contrast, changes induced by tyrosine-ring-$d_4$ labeling were barely detectable where the isotope-sensitive bands are expected. Both isotope substitutions had large effects on $P_M$ minus oxidized difference spectra. A prominent trough at 1542 $cm^{-1}$ was shifted to 1527 $cm^{-1}$ with $^{15}N$ labeling, and its magnitude was diminished with the appearance of a 1438 $cm^{-1}$ trough with tyrosine-ring-$d_4$ labeling. Both isotope substitutions also had large effects on a 1314 $cm^{-1}$ trough in the same spectra. These shifts indicate that the bands are linked to both a nitrogenous compound and a tyrosine, the most obvious candidate being the covalent histidine−tyrosine ligand of $Cu_B$. Comparison with model material data suggests that the tyrosine hydroxyl group is protonated when the binuclear center is oxidized but deprotonated in the $P_M$ intermediate. Positive bands at 1519 and 1570 $cm^{-1}$ were replaced with bands at 1504 and 1556 $cm^{-1}$, respectively, with tyrosine-ring-$d_4$ labeling, are characteristic of $\upsilon_{7a}$(C−O) and $\upsilon$(C−C) bands of neutral phenolic radicals, and most likely reflect the formation of the neutral radical state of the histidine−tyrosine ligand in $P_M$.

Structures of mitochondrial and bacterial cytochrome *c* oxidases have been determined at atomic resolution (*1*−*3*) and provide a wealth of structure−function information. Nevertheless, major questions about the chemical nature of important intermediates and their associated protonation changes remain. The catalytic cycle is thought to include "peroxy" (P)[1] and "ferryl" (F) intermediates (cf. ref *4*) that were first described in reversed electron transfer studies using coupled mitochondria (*5*, *6*), and which have been observed as transients in the forward reaction of fully reduced cytochrome *c* oxidase with oxygen (*7*−*10*). In the visible region, P and F of the bovine enzyme are characterized by distinct peaks at 607 nm (610 nm in *Paracoccus denitrificans*) and near 580 nm, respectively, but in the Soret region, both exhibit a similar red shift relative to the oxidized (O) state (*11*).

P or F can be formed from the O form when the enzyme has reacted with oxygen after receiving from an external donor two or three reducing equivalents, respectively (*12*). For example, reaction of the two-electron-reduced ("mixed-valence") enzyme with $O_2$ results in a 607 nm species, originally called Compound C (*13*). Incubation of the oxidized enzyme at high pH with CO and oxygen results in the same species (*14*), presumably by a two-electron reduction by CO, followed by reaction of the mixed-valence product with oxygen. This species has been termed $P_M$ to distinguish it from the related 607 nm P state ($P_R$) that is formed transiently when oxygen reacts with the fully reduced enzyme (*15*−*18*). $P_R$ differs from $P_M$ in that the binuclear center contains an additional electron that is donated by heme *a* (*7*, *19*).

† This work was funded by grants from the Wellcome Trust (Grant 062827) to P.R.R. and the Academy of Finland (Programs 44895 to M.W. and 42739 to A.P.).

* To whom correspondence should be addressed: Glynn Laboratory of Bioenergetics, Department of Biology, University College London, Gower Street, London WC1E 6BT, U.K. Telephone and fax: (+44) 20 7679 7746. E-mail: prr@ucl.ac.uk.

‡ University College London.

§ University of Helsinki.

[1] Abbreviations: ATR-FTIR, attenuated total reflection-Fourier transform infrared. Enzyme nomenclature follows: O, fully oxidized; R, fully reduced; P, 607 nm species; $P_M$, stable P species formed when the mixed-valence enzyme reacts with oxygen; $P_R$, transient P species with one more electron in the vicinity of the binuclear center in comparison to $P_M$; F, 580 nm ferryl species that is isoelectronic with $P_R$; $Yd_4$, tyrosine with all four ring hydrogens replaced with deuterons.

10.1021/bi048545j CCC: $27.50 
Published on Web 10/15/2004

Spectroscopic features of F are characteristic of a ferryl−cupric compound. P was suggested initially to have a peroxide structure, but a number of studies have now provided very strong evidence (*20*, *21*) that the O−O bond is already broken in P so that this species also has a ferryl−cupric structure, including magnetic circular dichroism data (*22*), Raman data on the iron−oxygen stretch frequency (*23*−*25*), and the observation of release of half of the labeled oxygen as water when P is formed with $^{18}O_2$ (*26*). Formation of a ferryl−cupric species from the oxidized ferric−cupric state involves breakage of the O−O bond with four electrons. For the F species, three are provided by an external reductant and one is from the ferric iron. In the case of $P_M$ formation, two electrons are provided from external sources and a third is from ferric iron. The fourth electron must come from within the protein, possibly from the covalent histidine−tyrosine ligand to $Cu_B$, which would form a radical state (*2*, *27*−*32*). However, this supposed radical cannot be detected by EPR spectroscopy (*33*, *34*), presumably due to spin coupling with oxidized $Cu_B$, and its protonation state also remains uncertain.

Fourier transform infrared (FTIR) spectroscopy has been used extensively to probe structural changes in individual cofactors and amino acids in proteins. Light-induced perturbation has been exploited to provide intricate atomic detail of systems such as bacteriorhodopsin (*35*, *36*) and photosynthetic reaction centers (*37*, *38*). Introduction of spectroelectrochemical cells (*39*), together with induction of redox changes with photochemicals, has allowed extension of FTIR redox difference spectroscopy to cytochrome *c* oxidase (*40*−*45*), complex I (*46*), the $bc_1$ complex (*47*), and other redox proteins (*48*). Interpretation of oxidase redox IR difference spectra has been aided by mutagenesis (*41*, *44*) and studies of effects of labeling with [$^{13}$C]propionate (*49*), ring-$d_4$ tyrosine (*50*), and [$^{15}$N]histidine and $^{15}$N global labeling (*51*). An alternative to transmission methods is attenuated total reflection (ATR)-FTIR spectroscopy (*52*, *53*), a method that has been applied to various proteins, including rhodopsin, bacteriorhodopsin (*54*), the nicotinic acetylcholine receptor (*55*), cytochrome oxidase (*56*−*60*), the $bc_1$ complex (*61*, *62*), and reaction centers (*63*). Its flexibility has allowed the IR features of the $P_M$ and F intermediates of bovine and bacterial oxidases to be probed (*58*, *59*). These studies are extended here by studies of effects of pH and isotope labeling on redox IR difference spectra of cytochrome *c* oxidase from *P. denitrificans*.

## MATERIALS AND METHODS

*Bacterial Growth and Enzyme Purification. P. denitrificans* was grown in succinate minimal medium (*64*). For universal $^{15}$N labeling, growth media contained [$^{15}$N]ammonium chloride (ICON Isotopes) as the sole nitrogen source. Tyrosine-ring-$d_4$ (ICON Isotopes) labeling was achieved as described in ref *29*. Cytochrome $aa_3$-type oxidase was prepared from unlabeled and labeled cultures as described in ref *65*. It was dissolved in 20 mM Tris-HCl and 0.05% (w/v) $\beta$-dodecyl maltoside at pH 7.8 and stored at 77 K until it was required.

*Film Preparation*. Production of stable films for ATR-FTIR measurements required depletion of the detergent content so that the sample became sufficiently hydrophobic. Oxidase (10−20 $\mu$L from a 100−200 $\mu$M stock) was diluted in 20 mM potassium phosphate buffer (pH 8.5) and pelleted by centrifugation. The pellet was homogenized in the same buffer containing 0.02% (w/v) sodium cholate and 0.02% (w/v) octyl glucoside and again pelleted by centrifugation. This was repeated four times with detergent-free phosphate buffer. Finally, the "ATR-ready" material was dispersed in 10−20 $\mu$L of distilled water and stored if necessary at −80 °C. Film preparation and rehydration on the ATR Si prism (3 mm diameter, three bounce, SensIR Europe) were essentially as described previously (*59*).

*ATR-FTIR Measurements.* The rehydrated film was covered by a chamber that allowed buffers to be perfused over the film surface and visible absolute and difference absorption changes to be recorded synchronously with IR changes, as detailed in refs *58* and *59*. Quantitation of forms was assessed from visible spectra using the relative extinction coefficients given for the bovine oxidase in ref *11* and assuming that the spectrum of the $P_M$ form of *P. denitrificans* oxidase is uniformly red-shifted by 3 nm relative to the bovine one. ATR-FTIR spectra were recorded simultaneously with a Bruker ISF 66/S spectrometer, fitted with a liquid nitrogen-cooled MCT-A detector. All quoted frequencies are accurate to $\pm 1$ cm$^{-1}$. Typically, 2000−3000 interferograms at 4 cm$^{-1}$ resolution were averaged over 270−400 s before Fourier tranformation into spectra and batches of spectra were further averaged to produce the spectra that are shown. Where necessary, baseline corrections due to protein swelling and/or shrinkage were made.

*Generation of Difference Spectra*. Degassed buffer [200 mM CHES, 20 mM potassium phosphate, and 200 mM KCl (pH 9.0) or 200 mM potassium phosphate and 200 mM KCl (pH 6.5)] was used as the perfusant throughout. To ensure that the oxidase was in the "fast" oxidized state, a cycle of reduction and reoxidation of the protein film was first performed by perfusion with buffer containing 3 mM sodium dithionite followed by one containing 1 mM potassium ferricyanide. To generate $P_M$, this was followed by perfusion with buffer at pH 9.0 containing 1 mM ferricyanide and which had been bubbled briefly with CO gas. Due to the difficulty with the removal of CO from the sample that was once exposed to CO and oxygen, new samples were used for each run. To improve the signal-to-noise ratio, typically individual spectra were calculated from 4000 averaged interferograms, and spectra from six different samples were averaged to produce the spectra that are shown. All measurements were taken at room temperature with a flow rate of 1.5 mL/min.

*Sample Quality Control.* As in previous studies (*59*), the major criterion used to assess sample integrity was to generate at the end of the experiment the CO-ligated reduced state by perfusion with buffer containing dithionite and CO and to ensure that these absolute spectra contained predominantly the form due to CO bound to the heme $a_3$ iron at 1965 cm$^{-1}$ with a half-peak width of 7 cm$^{-1}$ and with only smaller amounts of broader $\beta$ forms (*66*). These different forms were quantitated at the end of experiments by the level of formation of the reduced CO compound and deconvolution of the bands due to bound CO into a set of Gaussian components whose areas were integrated to provide relative concentrations. The levels of these $\beta$ forms were independent of pH and always less than 25% of the total integrated area.

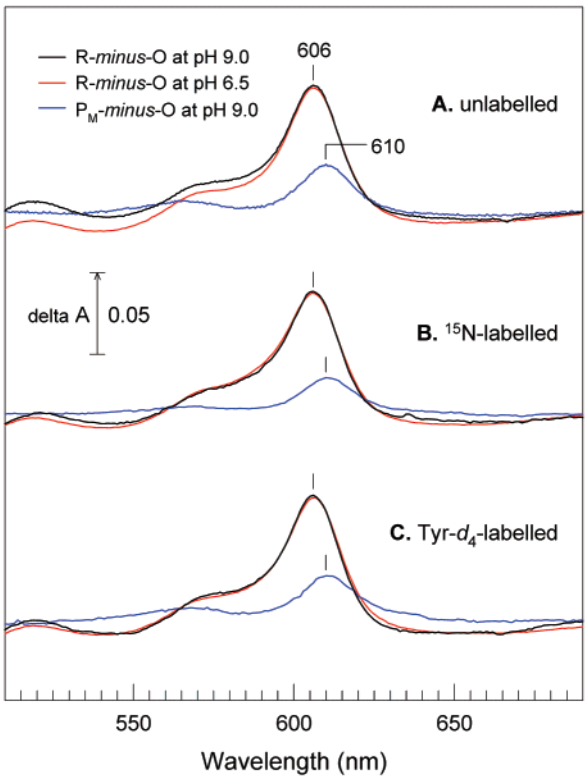


FIGURE 1: Perfusion-induced visible difference spectra of *P. denitrificans* cytochrome *c* oxidase. The figure shows reduced minus oxidized difference spectra for unlabeled (A), $^{15}$N-labeled (B), and Y$d_4$-labeled (C) forms at pH 9.0 (black) and pH 6.5 (red). These represent the difference between spectra recorded during perfusion with 3 mM sodium dithionite and a background recorded during perfusion with 1 mM potassium ferricyanide and are the average of 10 redox transitions. Also shown (blue) are $P_M$ minus O difference spectra induced by $CO/O_2$ perfusion. Background spectra were recorded during perfusion with 1 mM ferricyanide, and sample spectra were recorded after perfusion for 5 min with the same aerobic buffer that had been bubbled briefly with CO. Data are the average of six transitions, each from a fresh sample. Trace A at pH 9.0 was taken from ref *59*.

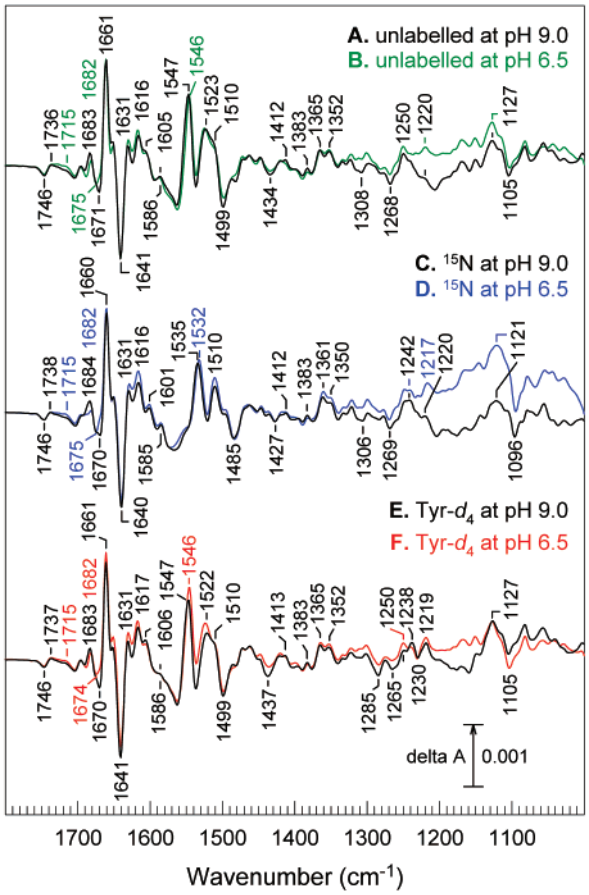


FIGURE 2: R minus O ATR-FTIR difference spectra. Spectra were recorded concurrently with the corresponding visible difference spectra of Figure 1. Spectra are of the unlabeled enzyme at pH 9.0 (A) and 6.5 (B), the $^{15}$N-labeled enzyme at pH 9.0 (C) and pH 6.5 (D), and the Y$d_4$-labeled enzyme at pH 9.0 (E) and pH 6.5 (F). Typically, spectra shown are averages of 60 individual spectra, each an average of 1000 interferograms, from six different samples. Trace A was taken from ref *59* and includes an extended region at 1200−1000 cm$^{-1}$. Where necessary, small baseline drifts due to swelling or shrinkage of the protein were subtracted.

## RESULTS AND DISCUSSION

*Visible Spectra during Reduction and Oxidation and Intermediate Formation.* Oxidase films were initially reduced with a perfusion buffer containing 3 mM sodium dithionite and scanned versus a clean prism surface as a background to produce reduced state absolute visible spectra (not shown). Samples were scanned again after reoxidation with an aerobic buffer containing 1 mM potassium ferricyanide. The resulting reduced minus oxidized difference spectra are shown in Figure 1. Unlabeled, $^{15}$N-labeled, and Tyr-ring-$d_4$ (Y$d_4$)-labeled oxidases all exhibited the characteristic peak at 606 nm at both pH 9.0 and 6.5. Although a "slow" form (*67*) of the *P. denitrificans* oxidase has yet to be identified, it is clear that the chloride-ligated state (*68*, *69*) does form. This "pulsing" procedure ensured that the samples were predominantly in the fast CO-reactive oxidized form, even if some formation of the chloride-ligated state or conversion to slow forms had occurred during sample handling, and so maximized the extent of reactivity with $CO/O_2$ to form $P_M$ in the subsequent steps (*67*). Quantitation versus absolute spectra indicated that more than 90% of the sample was redox-active.

For generation of the $P_M$ intermediate, background spectra of the fast oxidized form were recorded and the buffer was changed to one that had been bubbled briefly with CO gas. All forms over several minutes developed a band in their difference spectra at 610 nm (Figure 1) that is characteristic of the $P_M$ intermediate (*59*). Quantitation versus reduced minus oxidized difference spectra indicated approximately 90% conversion to $P_M$ in all cases.

*IR Difference Spectra during Reduction and Oxidation.* Reduced minus oxidized IR difference spectra in preparations at pH 9.0 and 6.5 were recorded by re-reduction after the reduction−reoxidation transition described above. The resulting spectra of the unlabeled enzyme (Figure 2A) are consistent with previously reported data on oxidases from *P. denitrificans* (*41*, *45*, *56*) and similar to spectra from other sources (*42*, *50*, *58*, *59*, *70*, *71*). The spectra were remarkably insensitive to pH change from pH 9.0 to 6.5, except for small differences around 1715 and 1675 cm$^{-1}$ that were observed consistently in unlabeled and labeled proteins (Figure 2B,C).

The spectra are dominated by changes in the 1700−1600 and 1570−1500 cm$^{-1}$ regions where amide I and II backbone changes occur, respectively, but some bands in these regions can also be tentatively assigned to vibrations of the heme rings and their substituents, including positive heme $a_3$ formyl bands in the 1661−1641 cm$^{-1}$ region that are obscured by

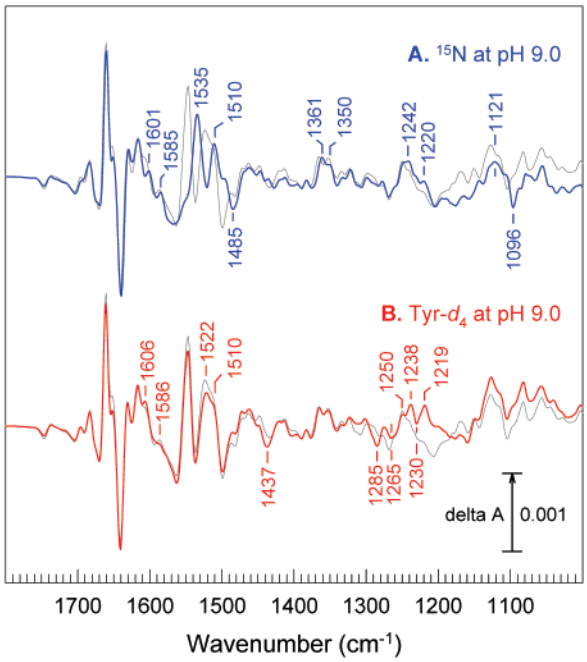


FIGURE 3: Effects of isotope labeling on R minus O ATR-FTIR difference spectra. For ease of comparison, data at pH 9.0 from Figure 2 have been overlaid on the R minus O difference spectrum of the unlabeled enzyme (trace A of Figure 2, gray): trace A, blue, $^{15}$N-labeled enzyme (same as trace C of Figure 2), and trace B, red, Y$d_4$-labeled enzyme (same as trace E of Figure 2).

overlapping amide I changes, a positive heme *a* formyl band at 1631 cm$^{-1}$, and a heme vinyl band at 1616−1617 cm$^{-1}$ (*56*, *72*−*75*). Small but consistent pH-sensitive and isotope-insensitive changes can be seen around 1680 cm$^{-1}$ (see also Figure 3). It seems likely that these are due to changes of heme propionic acid, at least one of which has been suggested to be protonated at pH 7 and with a band at 1676 cm$^{-1}$ (*49*). Likely heme ring mode changes are also evident at 1440−1400, 1365−1350, and 1250−1210 cm$^{-1}$ (*48*, *51*, *56*, *73*−*77*).

Important in this context is the 1750−1700 cm$^{-1}$ region where protonated carboxylic acids absorb strongly. The R minus O spectrum in the unlabeled enzyme showed a change at 1746/1736 cm$^{-1}$ (Figure 2 and ref *59*) that appears from its symmetry to arise from perturbation of a single group. Work from several groups with mutant forms of bacterial oxidases has shown clearly that features in this region arise predominantly from the protonated form of the equivalent of Glu-278 (*41*, *44*, *71*, *78*, *79*). Its insensitivity to Y$d_4$ labeling and to a pH change between pH 9.0 and 6.5 is consistent with reports of Hellwig *et al*. (*50*) and, together with its 5 cm$^{-1}$ downshift on H−D exchange (*59*) and the insensitivity to $^{15}$N labeling shown here, is consistent with this assignment and indicates that its p*K* is above 9 in both reduced and oxidized states (*45*, *59*, *80*). The same region of the equivalent IR difference spectrum of bovine oxidase has bands that must arise from perturbation of at least two carboxylic acid groups (*45*, *56*). It is possible that the redox-linked carboxylic region of the *P. denitrificans* oxidase also reflects change of more than one residue (*41*), with indications of an additional isotope-insensitive positive change around 1715 cm$^{-1}$ appearing in the pH 6.5 difference spectra of Figure 2.

$^{15}$N labeling caused large changes around 1560−1480 cm$^{-1}$ (Figure 3A). This is expected since the region is dominated by amide II vibrations that are downshifted by $^{15}$N labeling. However, strong bands from heme can contribute to this region (*48*), and Raman data indicate that their $^{15}$N-induced downshifts are less than 2 cm$^{-1}$ (*81*). Hence, underlying heme bands may account for the fact that large signals remain in the $^{15}$N-labeled sample. Downshifts of a 1605 cm$^{-1}$ shoulder (−4 cm$^{-1}$), a trough at 1434 cm$^{-1}$ (−7 cm$^{-1}$), and peaks at 1365 cm$^{-1}$ (−4 cm$^{-1}$) and 1352 cm$^{-1}$ (−2 cm$^{-1}$) appear. Their origins are at present unclear, although a good case has been made recently for assignment of the 1365 and 1352 cm$^{-1}$ bands to heme modes (*51*). Effects of Y$d_4$ labeling were difficult to detect with confidence (Figure 3B). Free tyrosine in its protonated state has major Y$d_4$ labeling-sensitive bands at 1599, 1518, 1455, and 1249 cm$^{-1}$ (*50*, *82*). Small changes are evident in these regions that might reasonably be assigned to the protonated tyrosine component. Some similar small changes were also reported by Hellwig *et al*. (*50*) in their Y$d_4$-labeled protein. No major changes in bands in the 1800−1615 cm$^{-1}$ region occurred with either isotope substitution.

Bands arising from ring C−N bonds of histidine are expected around 1100 cm$^{-1}$ (*83*−*85*), a region free of other major amino acid contributions. A trough at 1105 cm$^{-1}$ in the unlabeled enzyme was downshifted by around 9 cm$^{-1}$ by $^{15}$N labeling but was insensitive to Y$d_4$ labeling. A similar downshift was reported recently in equivalent redox difference specrta of oxidase from *Rhodobacter sphaeroides* with global $^{15}$N and $^{15}$N histidine labeling (*51*). This frequency is within the 1103−1112 cm$^{-1}$ range found for the C5−N1 bond of metal-bound histidine in its neutral (protonated) form (*83*) and suggests, as pointed out in refs *51* and *56*, that it arises from perturbation of one or more of the histidine ligands to $Cu_B$ and/or heme *a* and $a_3$ that are bonded through their N$\pi$ atoms with the free N$\tau$ position protonated (*2*, *86*).

*$P_M$ minus O IR Difference Spectra*. IR spectra were recorded (Figure 4) synchronously with the visible spectra that showed 90% formation of $P_M$ at 610 nm on perfusion with CO and $O_2$ (Figure 1). To improve the signal-to-noise ratio, typically 24 000 interferograms obtained from six different samples were averaged to produce the spectra that are shown. These $P_M$ minus O difference spectra are distinctly different from the R minus O difference spectra. $P_M$ minus O difference spectra of unlabeled forms of bovine and bacterial cytochrome *c* oxidases in $D_2O$ and $H_2O$ have been reported for the 1800−1200 cm$^{-1}$ region (*58*, *59*, *87*). The major features are in general accord, but assignments have remained speculative. Data in Figure 4 extend the analysis to 1000 cm$^{-1}$ and to further isotope effects. Although the 1700−1620 cm$^{-1}$ region will contain amide I changes, the strong peak and trough at 1656 and 1647 cm$^{-1}$, respectively, most likely arise from heme $a_3$ formyl perturbations (*56*, *72*, *74*) and the very sharp positive band at 1609 cm$^{-1}$ most likely arises from heme $a_3$ vinyl perturbation (*56*, *72*). Their insensitivities to $^{15}$N or Y$d_4$ labeling are consistent with such assignments (Figure 3B). We have previously suggested (*59*) that the sharp H−D-insensitive band at 1480 cm$^{-1}$ (*59*) might represent a heme $a_3$ ferryl feature (*58*), although assignment to a tyrosine radical has also been suggested (see below). Other bands at 1401(+), around 1330(+)/1300(−), and 1220(+) cm$^{-1}$ are also likely to be redox-sensitive features

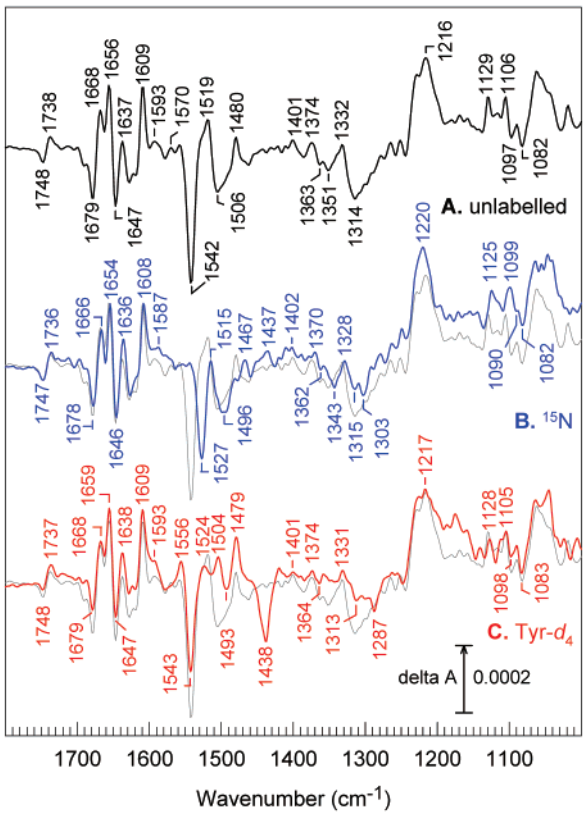


FIGURE 4: $P_M$ minus O ATR-FTIR difference spectra. Spectra were recorded concurrently with the corresponding visible difference spectra of Figure 1. $P_M$ minus O difference spectra for the transition from ferricyanide to ferricyanide and $CO/O_2$ at pH 9.0 were measured in unlabeled (A), $^{15}$N-labeled (B), and Y$d_4$-labeled (C) enzymes. Typically, spectra from six different samples were averaged, each of which was derived from 4000 averaged interferograms. Trace A was taken from ref *59* and includes an extended region at 1200−1000 cm$^{-1}$. Where necessary, small baseline drifts due to swelling or shrinkage of the protein were subtracted. For ease of comparison, the spectrum of the unlabeled enzyme (trace A, gray) is overlaid on traces B and C.

of heme $a_3$ (*48*, *56*, *73*−*77*).

Changes in the 1740 cm$^{-1}$ carboxylic acid region in $P_M$ that relax in F have been observed previously (*59*, *87*). In *R. sphaeroides* oxidase, they appeared as a trough with no clear associated peak and were interpreted in terms of glutamic acid deprotonation in $P_M$ (*87*). In the case of bovine and *P. denitrificans* oxidases (ref *59* and Figure 3), however, a relatively symmetrical 1748 cm$^{-1}$ trough and 1738 cm$^{-1}$ peak occur. Its downshift with H−D exchange (*59*) and its insensitivity to $^{15}$N or Y$d_4$ labeling (Figure 4) are consistent with a carboxylic acid origin but, as discussed previously (*59*), one that remains in its protonated state while undergoing an environmental or conformational change upon formation of $P_M$. The differences with data in ref *87* could mean that its p*K* in the $P_M$ form is below 8.5 in *R. sphaeroides*, whereas it is clearly above 9 in the *P. denitrificans* and bovine heart enzymes. Assignment to Glu-278 remains most likely on the basis of mutagenesis data (*41*, *44*, *71*, *78*, *79*), with the change associated with its central role in providing a pathway for intraprotein proton transfer for both proton translocation and, as now seems likely, delivery of a substrate proton to the oxygen reduction site (*88*−*93*).

In the region around 1100 cm$^{-1}$, where C−N stretching modes of histidine side chains are expected (*83*−*85*), two peaks at 1129 and 1106 cm$^{-1}$ in the unlabeled enzyme were downshifted by 4 and 7 cm$^{-1}$, respectively, upon $^{15}$N labeling, but were relatively insensitive to Y$d_4$ labeling. Their frequencies and isotope shifts are consistent with histidine changes, possibly representing a 1106 cm$^{-1}$ peak and 1090 cm$^{-1}$ trough arising from N$\pi$ protonation of an N$\tau$−metal-ligated hisitidine and a 1129 cm$^{-1}$ band arising from protonation of a free imidazolate residue (*83*, *85*). These intriguing possibilities could be investigated further by mutagenesis and specific labeling methods.

*Negative Features in the $P_M$ minus O Difference Spectra.* A particularly topical question about the chemistry of $P_M$ has concerned the role of the unusual covalently linked histidine−tyrosine ligand to $Cu_B$ that has been implicated as a proton and electron donor in the catalytic cycle (*30*, *94*−*96*), with the consensus expectation that this species becomes oxidized to a neutral radical in $P_M$ and re-reduced in F. However, no EPR signature could be found (*34*), and evidence for its existence remains indirect. Useful comparisons can be made with IR and Raman data on model materials related to tyrosine and the histidine−tyrosine ligand (*97*−*102*) and on tyrosine radical/tyrosine-OH IR difference spectra that can be generated in photosystem II (*103*). Tomson *et al.* (*102*) reported a band at 1546 cm$^{-1}$ in $D_2O$ that is associated uniquely with the histidine−tyrosine C−N linkage. This band, at 1549 cm$^{-1}$ in cytochrome *bo*$_3$, together with two others at 1483 and 1412 cm$^{-1}$, was downshifted with $^{15}$N labeling. In the same report, some rather weaker evidence was presented that Y$d_4$ labeling also caused a similar downshift in the 1549 cm$^{-1}$, but not the 1483 and 1412 cm$^{-1}$, bands. Hellwig *et al.* (*50*) reported prominent bands at 1547 and 1345 cm$^{-1}$ in a related model material in $H_2O$ that were lost when the phenolic group became deprotonated. When the radical state was generated from the deprotonated form, a band at 1303 cm$^{-1}$ was lost (*98*), although clear positive bands that might be assigned to the radical were not evident. A much larger database of IR and Raman features of neutral phenoxyl radical models and tyrosine radicals in photosystem II and other proteins is available (*103*), and these show two prominent modes of the neutral phenolic radical, $\upsilon$(C−C) at 1550−1610 cm$^{-1}$ and $\upsilon_{7a}$(C−O) at 1480−1530 cm$^{-1}$. Equivalent bands should occur in the histidine−tyrosine radical, though a Raman study (*99*) has emphasized the importance of the relative orientations of the phenolic and imidazole rings in governing the vibrational spectra of such compounds. Hence, in summary, a number of useful guiding features are available, but much remains to be established in terms of isotope shifts, vibrational properties of the radical state, and influences of metal chelation and relative ring orientations on spectroscopic properties.

On the basis of model compound data, we have previously suggested that the 1542−1547 and 1314 cm$^{-1}$ troughs in the $P_M$ minus O IR difference spectra could be assigned to the deprotonation of the phenolic group of the histidine−tyrosine ligand when going from the oxidized to the $P_M$ state. The data presented here allow extension of this analysis. Upon $^{15}$N labeling, the trough at 1542 cm$^{-1}$ was downshifted by 15 cm$^{-1}$, consistent with data in ref *102* and showing that it is associated with a nitrogenous element. Y$d_4$ labeling caused a decrease in the amplitude of the 1542 cm$^{-1}$ trough together with a prominent new trough at 1438 cm$^{-1}$. Data

in ref *102* suggest that Y$d_4$ labeling should downshift the 1542 cm$^{-1}$ band by only 9−13 cm$^{-1}$, although labeling of free tyrosine-OH results in the loss of the 1518 cm$^{-1}$ $\upsilon_{19}$(C−C) band and appearance of a new band at 1416 cm$^{-1}$. In $Y_D^{\bullet}/Y_DOH$ difference spectra of photosystem II, this labeling results in replacement of a trough around 1490 cm$^{-1}$ with one at 1428 cm$^{-1}$ (*104*). Hence, while it is not clear if the 1438 cm$^{-1}$ trough in our $P_M$ minus O spectra arises from a shift of part of the 1542 cm$^{-1}$ trough or, perhaps, from a downshift of the trough at 1490 cm$^{-1}$, it is clear that all are associated with a tyrosine residue. The partial retention of the 1542 cm$^{-1}$ band with Y$d_4$ labeling may arise because an amide II component contributes to the region, because Y$d_4$ labeling was incomplete (cf. ref *50*), or because this vibration is relatively insensitive to Y$d_4$ labeling. Both isotope substitutions also had large effects on the 1314 cm$^{-1}$ trough, in both cases being diminished and, in the case of Y$d_4$ labeling, causing the appearance of a new trough at 1287 cm$^{-1}$. This might again find an analogy in the $Y_D^{\bullet}/Y_DOH$ difference spectra where Y$d_4$ labeling causes a 24 cm$^{-1}$ downshift of a band at 1250 cm$^{-1}$ (*104*). Overall, therefore, the data support the assignment of the 1542 and 1314 cm$^{-1}$ troughs to the histidine−tyrosine structure. On the basis of pH effects on model materials and comparisons with $Y_D^{\bullet}/Y_DOH$ difference spectra, it is most likely that the O state has a protonated tyrosine, though we cannot at this stage fully rule out a tyrosinate that is so strongly hydrogen bonded by an adjacent group that the system loses its negatively charged character. The assignment might be also supported by the behavior of a 1351 cm$^{-1}$ trough, which was downshifted with $^{15}$N labeling and appeared to be absent with Y$d_4$ labeling, since a 1345 cm$^{-1}$ band was also reported in the histidine−tyrosine model compound in ref *50*.

*Positive Features in the $P_M$ minus O Difference Spectra*. The model compound and photosystem II data can also guide analyses of positive bands in terms of whether a neutral histidine−tyrosine radical is produced in $P_M$. A Raman band at 1489 cm$^{-1}$ was identified in the $P_M$ state produced by reaction of hydrogen peroxide with bacterial cytochrome *bo*, and it was tentatively assigned to a tyrosine radical, rather than a heme, origin (*32*). In addition, Nyquist *et al*. (*87*) suggested that a 1479 cm$^{-1}$ band in their $P_M$ minus O IR difference spectra of cytochrome *c* oxidase from *R. sphaeroides* might arise from a tyrosine radical (together with bands at 1587, 1528, and 1517 cm$^{-1}$; see below). In a previous study, we observed that the 1480 cm$^{-1}$ peak persisted in the F state (albeit at lower intensity in the *Paracoccus* enzyme), a state in which a radical should not occur (*59*). Global $^{15}$N labeling downshifted it, or perhaps split it into two bands at 1467 and 1437 cm$^{-1}$, but Y$d_4$ labeling had little effect. Hence, although the isotope labeling (which also labels the heme) is consistent with, but cannot yet confirm, its ferryl origin, it seems certain that the 1480 cm$^{-1}$ band is not specific for the $P_M$ state and cannot arise from tyrosine residues. Likewise, most of the band seen near 1590 cm$^{-1}$ (ref *87* and Figure 3) does not appear to be associated with the histidine−tyrosine dimer because it is hardly affected by $^{15}$N or Y$d_4$ labeling.

However, the $P_M$ minus O spectra do have a positive band at 1519 cm$^{-1}$ and a smaller peak at around 1570 cm$^{-1}$ that are unaffected by H−D exchange and do not persist in F (*59*). It seems likely that the 1519 cm$^{-1}$ and, with less confidence, the small 1570 cm$^{-1}$ band may well be equivalent to the 1517 and 1587 cm$^{-1}$ bands, respectively, of Nyquist *et al*. (*87*). In addition, their positive band at 1528 cm$^{-1}$ may correspond to a shoulder at that frequency in our spectrum (Figure 3), and to the peak at 1530 cm$^{-1}$ reported in our earlier study (*59*). However, this latter feature persists in the F state (*59*, *87*) and is therefore unlikely to arise from a putative histidine−tyrosine radical. Distinct positive bands in the Y$d_4$-labeled enzyme are seen at 1504 and 1556 cm$^{-1}$ and may be the downshifted positions of the 1519 and 1570 cm$^{-1}$ peaks, respectively, in the unlabeled protein. The effects of global $^{15}$N labeling are less clear due to overlapping signals. Interestingly, the $\upsilon_{7a}$(C−O) and $\upsilon$(C−C) bands of neutral phenoxy radicals, and of neutral tyrosine radicals in photosystem II (see above), are expected to appear in this region. Since these bands are, moreover, unique for the $P_M$ state (*59*, *87*), it therefore seems likely that they do indeed arise from a neutral radical form of the histidine−tyrosine dimer in the active site.

## CONCLUSIONS

In summary, these data provide a range of more solid assignments for features of redox and $P_M$ minus O IR difference spectra in terms of heme and amino acid changes. The data strengthen the assignment of the change around 1740 cm$^{-1}$ in $P_M$ minus O spectra to a protonated carboxylic acid, which by comparison with mutagenesis data from other laboratories (*41*, *44*, *71*, *78*, *79*, *87*) is probably Glu-278, the environment of which changes in $P_M$ but whose p*K* remains above 9 in $P_M$. Histidine perturbations around 1100 cm$^{-1}$ are also documented for the first time. The data strongly suggest that the covalent histidine−tyrosine linkage, although equivocal in the crystallographic data of the *P. denitrificans* enzyme (*27*), is indeed present, in agreement with direct chemical analyses (*105*). The p*K* of its tyrosine hydroxyl in the oxidized and reduced enzyme must be well above the p*K* of 8.3−9.2 reported for this group in related model compounds in aqueous media (*98*−*100*). Bands suggestive of its conversion to its neutral radical state in the $P_M$ state have also been identified. It should be possible to specify further atomic details of the chemical and protonation changes of $P_M$ and other intermediates by development of the isotope labeling studies both in oxidase and in related model compounds.

## ACKNOWLEDGMENT

We are grateful to Mr. Santiago Garcia for specialist electronic and mechanical support.

## REFERENCES

1. Iwata, S., Ostermeier, C., Ludwig, B., and Michel, H. (1995) Structure at 2.8 Å resolution of cytochrome *c* oxidase from *Paracoccus denitrificans*, *Nature 376*, 660−669.
2. Yoshikawa, S., Shinzawa-Itoh, K., Nakashima, R., Yaono, R., Yamashita, E., Inoue, N., Yao, M., Fei, M. J., Libeu, C. P., Mizushima, T., Yamaguchi, H., Tomizaki, T., and Tsukihara, T. (1998) Redox-coupled crystal structural changes in bovine heart cytochrome *c* oxidase, *Science 280*, 1723−1729.
3. Svensson-Ek, M., Abramson, J., Larsson, G., Törnroth, S., Brzezinski, P., and Iwata, S. (2002) The X-ray crystal structures of wild-type and EQ(I-286) mutant cytochrome *c* oxidases from *Rhodobacter sphaeroides*, *J. Mol. Biol. 321*, 329−339.

4. Babcock, G. T., and Wikström, M. (1992) Oxygen activation and the conservation of energy in cell respiration, *Nature 356*, 301−309.
5. Wikström, M. (1981) Energy-dependent reversal of the cytochrome oxidase reaction, *Proc. Natl. Acad. Sci. U.S.A. 78*, 4051−4054.
6. Wikström, M., and Morgan, J. E. (1992) The dioxygen cycle. Spectral, kinetic, and thermodynamic characteristics of ferryl and peroxy intermediates observed by reversal of the cytochrome oxidase reaction, *J. Biol. Chem. 267*, 10266−10273.
7. Morgan, J. E., Verkhovsky, M. I., and Wikstrom, M. (1996) Observation and assignment of peroxy and ferryl intermediates in the reduction of dioxygen to water by cytochrome *c* oxidase, *Biochemistry 35*, 12235−12240.
8. Sucheta, A., Georgiadis, K. E., and Einarsdóttir, O. (1997) Mechanism of cytochrome *c* oxidase-catalyzed reduction of dioxygen to water: evidence for peroxy and ferryl intermediates at room temperature, *Biochemistry 36*, 554−565.
9. Morgan, J. E., Verkhovsky, M. I., Puustinen, A., and Wikström, M. (1995) Identification of a "peroxy" intermediate in cytochrome $bo_3$ of *Escherichia coli*, *Biochemistry 34*, 15633−15637.
10. Lauraeus, M., Morgan, J. E., and Wikström, M. (1993) Peroxy and ferryl intermediates of the quinol-oxidizing cytochrome $aa_3$ from *Bacillus subtilis*, *Biochemistry 32*, 2664−2670.
11. Rich, P. R., and Moody, A. J. (1997) in *Bioelectrochemistry: principles and practice* (Gräber, P., and Milazzo, G., Eds.) pp 419−456, Birkhäuser Verlag AG, Basel, Switzerland.
12. Verkhovsky, M. I., Morgan, J. E., and Wikström, M. (1996) Redox transitions between oxygen intermediates in cytochrome-*c* oxidase, *Proc. Natl. Acad. Sci. U.S.A. 93*, 12235−12239.
13. Chance, B., Saronio, C., and Leigh, J. S. (1975) Functional intermediates in the reaction of membrane-bound cytochrome oxidase with oxygen, *J. Biol. Chem. 250*, 9226−9237.
14. Nicholls, P., and Chanady, G. A. (1981) Interactions of cytochrome $aa_3$ with oxygen and carbon monoxide. The role of the 607 nm complexes, *Biochim. Biophys. Acta 634*, 256−265.
15. Verkhovsky, M. I., Morgan, J. E., and Wikström, M. (1994) Oxygen binding and activation: early steps in the reaction of oxygen with cytochrome *c* oxidase, *Biochemistry 33*, 3079−3086.
16. Ädelroth, P., Ek, M., and Brzezinski, P. (1998) Factors determining electron-transfer rates in cytochrome *c* oxidase: investigation of the oxygen reaction in the *R. sphaeroides* enzyme, *Biochim. Biophys. Acta 1367*, 107−117.
17. Sucheta, A., Szundi, I., and Einarsdóttir, O. (1998) Intermediates in the reaction of fully reduced cytochrome *c* oxidase with dioxygen, *Biochemistry 37*, 17905−17914.
18. Karpefors, M., Ädelroth, P., Namslauer, A., Zhen, Y., and Brzezinski, P. (2000) Formation of the "peroxy" intermediate in cytochrome *c* oxidase is associated with internal proton/hydrogen transfer, *Biochemistry 39*, 14664−14669.
19. Morgan, J. E., Verkhovsky, M. I., Palmer, G., and Wikström, M. (2001) The role of the $P_R$ intermediate of cytochrome *c* oxidase with $O_2$, *Biochemistry 40*, 6882−6892.
20. Fabian, M., and Palmer, G. (1995) The interaction of cytochrome oxidase with hydrogen peroxide: The relationship of compounds P and F, *Biochemistry 34*, 13802−13810.
21. Fabian, M., and Palmer, G. (1999) Redox state of peroxy and ferryl intermediates in cytochrome *c* oxidase catalysis, *Biochemistry 38*, 6270−6275.
22. Watmough, N. J., Cheesman, M. R., Greenwood, C., and Thomson, A. J. (1994) Cytochrome *bo* from *Escherichia coli*: reaction of the oxidized enzyme with hydrogen peroxide, *Biochem. J. 300*, 469−475.
23. Proshlyakov, D. A., Ogura, T., Shinzawa-Itoh, K., Yoshikawa, S., Appelman, E. H., and Kitagawa, T. (1994) Selective resonance Raman observation of the "607 nm" form generated in the reaction of oxidized cytochrome *c* oxidase with hydrogen peroxide, *J. Biol. Chem. 269*, 29385−29388.
24. Proshlyakov, D. A., Ogura, T., Shinzawa-Itoh, K., Yoshikawa, S., and Kitagawa, T. (1996) Microcirculating system for simultaneous determination of Raman and absorption spectra of enzymatic reaction intermediates and its application to the reaction of cytochrome *c* oxidase with hydrogen peroxide, *Biochemistry 35*, 76−82.
25. Proshlyakov, D. A., Ogura, T., Shinzawa-Itoh, K., Yoshikawa, S., and Kitagawa, T. (1996) Resonance Raman/absorption characterization of the oxo intermediates of cytochrome *c* oxidase generated in its reaction with hydrogen peroxide: pH and $H_2O_2$ concentration dependence, *Biochemistry 35*, 8580−8586.
26. Fabian, M., Wong, W. W., Gennis, R. B., and Palmer, G. (1999) Mass spectrometric determination of dioxygen bond splitting in the "peroxy" intermediate of cytochrome *c* oxidase, *Proc. Natl. Acad. Sci. U.S.A. 96*, 13114−13117.
27. Ostermeier, C., Harrenga, A., Ermler, U., and Michel, H. (1997) Structure at 2.7 Å resolution of the *Paracoccus denitrificans* two-subunit cytochrome *c* oxidase complexed with an antibody $F_V$ fragment, *Proc. Natl. Acad. Sci. U.S.A. 94*, 10547−10553.
28. Mitchell, D. M., Ädelroth, P., Hosler, J. P., Fetter, J. R., Brzezinski, P., Pressler, M. A., Aasa, R., Malmström, B. G., Alben, J. O., Babcock, G. T., Gennis, R. B., and Ferguson-Miller, S. (1996) A ligand-exchange mechanism of proton pumping involving tyrosine-422 of subunit I of cytochrome oxidase is ruled out, *Biochemistry 35*, 824−828.
29. MacMillan, F., Kannt, A., Behr, J., Prisner, T., and Michel, H. (1999) Direct evidence for a tyrosine radical in the reaction of cytochrome *c* oxidase with hydrogen peroxide, *Biochemistry 38*, 9179−9184.
30. Michel, H. (1999) Proton pumping by cytochrome *c* oxidase, *Nature 402*, 602−603.
31. Proshlyakov, D. A., Pressler, M. A., DeMaso, C., Leykam, J. F., DeWitt, D. L., and Babcock, G. T. (2000) Oxygen activation and reduction in respiration: Involvement of redox-active tyrosine 244, *Science 290*, 1588−1591.
32. Uchida, T., Mogi, T., and Kitagawa, T. (2000) Resonance Raman studies of oxo intermediates in the reaction of pulsed cytochrome *bo* with hydrogen peroxide, *Biochemistry 39*, 6669−6678.
33. Rigby, S. E. J., Jünemann, S., Rich, P. R., and Heathcote, P. (2000) The reaction of hydrogen peroxide with bovine cytochrome *c* oxidase produces a tryptophan cation radical and a porphyrin cation radical, *Biochemistry 39*, 5921−5928.
34. Rich, P. R., Rigby, S. E. J., and Heathcote, P. (2002) Radicals associated with the catalytic intermediates of bovine cytochrome *c* oxidase, *Biochim. Biophys. Acta 1554*, 137−146.
35. Braiman, M. S., Mogi, T., Marti, T., Stern, L. J., Khorana, H. G., and Rothschild, K. J. (1988) Vibrational spectroscopy of bacteriorhodopsin mutants: light-driven proton transport involves protonation changes of asparatic acid residues 85, 96, and 212, *Biochemistry 27*, 8516−8520.
36. Gerwert, K., Hess, B., Soppa, J., and Oesterhelt, D. (1989) Role of aspartate-96 in proton translocation by bacteriorhodopsin, *Proc. Natl. Acad. Sci. U.S.A. 86*, 4943−4947.
37. Mäntele, W., Nabedryk, E., Tavitian, B. A., Kreutz, W., and Breton, J. (1985) Light-induced Fourier transform infrared (FTIR) spectroscopic investigations of the primary oxidation in bacterial photosynthesis, *FEBS Lett. 187*, 227−232.
38. Tabitian, B. A., Nabedryk, E., Mäntele, W., and Breton, J. (1986) Light-induced Fourier transform infrared (FTIR) spectroscopic investigations of primary reactions in photosystem I and photosystem II, *FEBS Lett. 201*, 151−157.
39. Moss, D., Nabedryk, E., Breton, J., and Mäntele, W. (1990) Redox-linked conformational changes in proteins detected by a combination of IR spectroscopy and protein electrochemistry. Evaluation of the technique with cytochrome *c*, *Eur. J. Biochem. 187*, 565−572.
40. Hellwig, P., Rost, B., Kaiser, U., Ostermeier, C., Michel, H., and Mäntele, W. (1996) Carboxyl group protonation upon reduction of the *Paracoccus denitrificans* cytochrome *c* oxidase: Direct evidence by FTIR spectroscopy, *FEBS Lett. 385*, 53−57.
41. Hellwig, P., Behr, J., Ostermeier, C., Richter, O.-M. H., Pfitzner, U., Odenwald, A., Ludwig, B., Michel, H., and Mäntele, W. (1998) Involvement of glutamic acid 278 in the redox reaction of the cytochrome *c* oxidase from *Paracoccus denitrificans* investigated by FTIR spectroscopy, *Biochemistry 37*, 7390−7399.
42. Lübben, M., and Gerwert, K. (1996) Redox FTIR difference spectroscopy using caged electrons reveals contributions of carboxyl groups to the catalytic mechanism of haem-copper oxidases, *FEBS Lett. 397*, 303−307.
43. Yamazaki, Y., Kandori, H., and Mogi, T. (1999) Effects of subunit I mutations on redox-linked conformational changes of the *Escherichia coli bo*-type ubiquinol oxidase revealed by Fourier transform infrared spectroscopy, *J. Biochem. 126*, 194−199.
44. Lübben, M., Prutsch, A., Mamat, B., and Gerwert, K. (1999) Electron-transfer induces side-chain conformational changes of glutamate-286 from cytochrome $bo_3$, *Biochemistry 38*, 2048−2056.
45. Hellwig, P., Soulimane, T., Buse, G., and Mäntele, W. (1999) Similarities and dissimilarities in the structure−function relation between the cytochrome *c* oxidase from bovine heart and from

*Paracoccus denitrificans* as revealed by FT-IR difference spectroscopy, *FEBS Lett. 458*, 83−86.
46. Hellwig, P., Scheide, D., Bungert, S., Mäntele, W., and Friedrich, T. (2000) FT-IR spectroscopic characterization of NADH:ubiquinone oxidoreductase (complex I) from *Escherichia coli*: oxidation of FeS cluster N2 is coupled with the protonation of an aspartate or glutamate side chain, *Biochemistry 39*, 10884−10891.
47. Baymann, F., Robertson, D. E., Dutton, P. L., and Mäntele, W. (1999) Electrochemical and spectroscopic investigations of the cytochrome $bc_1$ complex from *Rhodobacter capsulatus*, *Biochemistry 38*, 13188−13199.
48. Berthomieu, C., Boussac, A., Mäntele, W., Breton, J., and Nabedryk, E. (1992) Molecular changes following oxidoreduction of cytochrome *b*559 characterized by Fourier transform infrared difference spectroscopy and electron paramagnetic resonance: Photooxidation in photosystem II and electrochemistry of isolated cytochrome *b*559 and iron protoporphyrin IX-bisimidazole model compounds, *Biochemistry 31*, 11460−11471.
49. Behr, J., Hellwig, P., Mäntele, W., and Michel, H. (1998) Redox dependent changes at the heme propionates in cytochrome *c* oxidase from *Paracoccus denitrificans*: direct evidence from FTIR difference spectroscopy in combination with heme propionate $^{13}C$ labeling, *Biochemistry 37*, 7400−7406.
50. Hellwig, P., Pfitzner, U., Behr, J., Rost, B., Pesavento, P., Donk, W. v., Gennis, R. B., Michel, H., Ludwig, B., and Mäntele, W. (2002) Vibrational modes of tyrosine in cytochrome *c* oxidase from *Paracoccus denitrificans*: FTIR and electrochemical studies on Tyr-$D_4$-labeled and on Tyr280His and Tyr35Phe mutant enzymes, *Biochemistry 41*, 9116−9125.
51. Schmidt, B., Hillier, W., McCracken, J., and Ferguson-Miller, S. (2004) The use of stable isotopes and spectroscopy to investigate the energy transducing function of cytochrome *c* oxidase, *Biochim. Biophys. Acta 1655*, 248−255.
52. Goormaghtigh, E., Raussens, V., and Ruysschaert, J.-M. (1999) Attenuated total reflection infrared spectroscopy of proteins and lipids in biological membranes, *Biochim. Biophys. Acta 1422*, 105−185.
53. Heberle, J., and Zscherp, C. (1996) ATR/FT-IR difference spectroscopy of biological matter with microsecond time resolution, *Appl. Spectrosc. 50*, 588−596.
54. Zscherp, C., Schlesinger, R., Tittor, J., Oesterhelt, D., and Heberle, J. (1999) In situ determinatin of transient p$K_a$ changes of internal amino acids of bacteriorhodopsin by using time-resolved atenuated total reflection Fourier-transform infrared spectroscopy, *Proc. Natl. Acad. Sci. U.S.A. 96*, 5498−5503.
55. Baenziger, J. E., Miller, K. W., and Rothschild, K. J. (1993) Fourier transform infrared difference spectroscopy of the nicotinic acetylcholine receptor: evidence for specific protein structural changes upon desensitization, *Biochemistry 32*, 5448−5454.
56. Rich, P. R., and Breton, J. (2002) Attenuated total reflection Fourier transform infrared studies of redox changes in bovine cytochrome *c* oxidase: resolution of the redox Fourier transform infrared difference spectrum of heme $a_3$, *Biochemistry 41*, 967−973.
57. Nyquist, R. M., Heitbrink, D., Bolwien, C., Wells, T. A., Gennis, R., and Heberle, J. (2001) Perfusion-induced redox differences in cytochrome *c* oxidase: ATR/FT-IR spectroscopy, *FEBS Lett. 505*, 63−67.
58. Iwaki, M., Breton, J., and Rich, P. R. (2002) ATR-FTIR difference spectroscopy of the $P_M$ intermediate of bovine cytochrome *c* oxidase, *Biochim. Biophys. Acta 1555*, 116−121.
59. Iwaki, M., Puustinen, A., Wikström, M., and Rich, P. R. (2003) ATR-FTIR spectroscopy of the $P_M$ and F intermediates of bovine and *Paracoccus denitrificans* cytochrome *c* oxidase, *Biochemistry 42*, 8809−8817.
60. Iwaki, M., and Rich, P. R. (2004) Direct detection of formate ligation in cytochrome *c* oxidase by ATR-FTIR spectroscopy, *J. Am. Chem. Soc. 126*, 2386−2389.
61. Iwaki, M., Giotta, L., Akinsiku, A. O., Schägger, H., Fisher, N., Breton, J., and Rich, P. R. (2003) Redox-induced transitions in bovine cytochrome *bc*1 complex studied by perfusion-induced ATR-FTIR spectroscopy, *Biochemistry 42*, 11109−11119.
62. Iwaki, M., Osyczka, A., Moser, C. C., Dutton, P. L., and Rich, P. R. (2004) ATR-FTIR spectroscopy studies of ion-sulfur protein and cytochrome $c_1$ in the *Rhodobacter capsulatus* cytochrome $bc_1$ complex, *Biochemistry 43*, 9477−9486.
63. Iwaki, M., Andrianambinintsoa, S., Rich, P. R., and Breton, J. (2002) Attenuated total reflection Fourier transform infrared spectroscopy of redox transitions in photosynthetic reaction centers: comparison of perfusion- and light-induced difference spectra, *Spectrochim. Acta A58*, 1523−1533.
64. Ludwig, B. (1986) Cytochrome *c* oxidase from *Paracoccus denitrificans*, *Methods Enzymol. 126*, 153−159.
65. Riistama, S., Laakkonen, L., Wikström, M., Verkhovsky, M. I., and Puustinen, A. (1999) The calcium binding site in cytochrome $aa_3$ from *Paracoccus denitrificans*, *Biochemistry 38*, 10670−10677.
66. Park, S., Pan, L. P., Chan, S. I., and Alben, J. O. (1996) Photoperturbation of the heme $a_3$−$Cu_B$ binuclear center of cytochrome *c* oxidase CO complex observed by Fourier transform infrared spectroscopy, *Biophys. J. 71*, 1036−1047.
67. Moody, A. J. (1996) 'As prepared' forms of fully oxidised haem/Cu terminal oxidases, *Biochim. Biophys. Acta 1276*, 6−20.
68. Moody, A. J., Richardson, M., Spencer, J. P. E., Brandt, U., and Rich, P. R. (1994) '$CO_2$-ligated' cytochrome *c* oxidase: characterization and comparison with the $Cl^-$-ligated enzyme, *Biochem. J. 302*, 821−826.
69. Moody, A. J., Butler, C. S., Watmough, N. J., Thomson, A. J., and Rich, P. R. (1998) The reaction of halides with pulsed cytochrome *bo* from *Escherichia coli*, *Biochem. J. 331*, 459−464.
70. Hellwig, P., Soulimane, T., Buse, G., and Mäntele, W. (1999) Electrochemical, FTIR, and UV/VIS spectroscopic properties of the $ba_3$ oxidase from *Thermus thermophilus*, *Biochemistry 38*, 9648−9658.
71. Gennis, R. B. (2003) Some recent contributions of FTIR difference spectroscopy to the study of cytochrome oxidase, *FEBS Lett. 555*, 2−7.
72. Hellwig, P., Grzybek, S., Behr, J., Michel, H., and Mäntele, W. (1999) Electrochemical and ultraviolet/visible/infrared spectroscopic analysis of heme *a* and $a_3$ redox reactions in the cytochrome *c* oxidase from *Paracoccus denitrificans*: separation of heme *a* and $a_3$ contributions and assignment of vibrational modes, *Biochemistry 38*, 1685−1694.
73. Han, S., Ching, Y., Hammes, S. L., and Rousseau, D. L. (1991) Vibrational structure of the formyl group on heme *a*. Implications on the properties of cytochrome *c* oxidase, *Biophys. J. 60*, 45−52.
74. Ching, Y.-C., Argade, P. V., and Rousseau, D. L. (1985) Resonance Raman spectra of $CN^-$-bound cytochrome oxidase: spectral isolation of cytochromes $a^{2+}$, $a_3{}^{2+}$ and $a_3{}^{2+}$(CN), *Biochemistry 24*, 4938−4946.
75. Choi, S., Lee, J. J., Wei, Y. H., and Spiro, T. G. (1983) Resonance Raman and electronic spectra of heme *a* complexes of cytochrome oxidase, *J. Am. Chem. Soc. 105*, 3692−3707.
76. Alben, J. O. (1978) in *The Porphyrins* (Dolphin, D., Ed.) Vol. III, pp 323−345, Academic Press, London.
77. Argade, P. V., Ching, Y.-C., and Rousseau, D. L. (1986) Resonance Raman spectral isolation of the *a* and *a*3 chromophores in cytochrome oxidase, *Biophys. J. 50*, 613−620.
78. Puustinen, A., Bailey, J. A., Dyer, R. B., Mecklenburg, S. L., Wikström, M., and Woodruff, W. H. (1997) Fourier transform infrared evidence for connectivity between $Cu_B$ and glutamic acid 286 in cytochrome $bo_3$ from *E. coli*, *Biochemistry 36*, 13195−13200.
79. Rost, B., Behr, J., Hellwig, P., Richter, O. M. H., Ludwig, B., Michel, H., and Mäntele, W. (1999) Time-resolved FT-IR studies on the CO adduct of *Paracoccus denitrificans* cytochrome *c* oxidase: Comparison of the fully reduced and the mixed valence form, *Biochemistry 38*, 7565−7571.
80. Okuno, D., Iwase, T., Shinzawa-Itoh, K., Yoshikawa, S., and Kitagawa, T. (2003) FTIR detection of protonation/deprotonation of key carboxyl side chains caused by redox change of the Cu(A)−heme *a* moiety and ligand dissociation from the heme $a_3$−Cu(B) center of bovine heart cytochrome *c* oxidase, *J. Am. Chem. Soc. 125*, 7209−7218.
81. Hu, S. Z., Smith, K. M., and Spiro, T. G. (1996) Assignment of protoheme resonance Raman spectrum by heme labeling in myoglobin, *J. Am. Chem. Soc. 118*, 12638−12646.
82. Barth, A. (2000) The infrared absorption of amino acid side chains, *Prog. Biophys. Mol. Biol. 74*, 141−173.
83. Hasegawa, K., Ono, T.-A., and Noguchi, T. (2002) Ab initio density functional theory calculations and vibrational analysis of zinc-bound 4-methylimidazole as a model of a histidine ligand in metalloenzymes, *J. Phys. Chem. A 106*, 3377−3390.
84. Hasegawa, K., Ono, T.-A., and Noguchi, T. (2000) Vibrational spectra and ab initio DFT calculations of 4-methylimidazole and its different protonation forms: Infrared and Raman markers of

the protonation state of a histidine side chain, *J. Phys. Chem. B 104*, 4253−4265.
85. Berthomieu, C., and Hienerwadel, R. (2001) Iron coordination in photosystem II: interaction between bicarbonate and the $Q_B$ pocket studied by Fourier transform infrared spectroscopy, *Biochemistry 40*, 4044−4052.
86. Kannt, A., Lancaster, R. D., and Michel, H. (1998) The coupling of electron transfer and proton translocation: electrostatic calculations on *Paracoccus denitrificans* cytochrome *c* oxidase, *Biophys. J. 74*, 708−721.
87. Nyquist, R. M., Heitbrink, D., Bolwien, C., Gennis, R. B., and Heberle, J. (2003) Direct observation of protonation reactions during the catalytic cycle of cytochrome *c* oxidase, *Proc. Natl. Acad. Sci. U.S.A. 100*, 8715−8720.
88. Fetter, J. R., Qian, J., Shapleigh, J., Thomas, J. W., García-Horsman, A., Schmidt, E., Hosler, J., Babcock, G. T., Gennis, R. B., and Ferguson-Miller, S. (1995) Possible proton relay pathways in cytochrome *c* oxidase, *Proc. Natl. Acad. Sci. U.S.A. 92*, 1604−1608.
89. Wikström, M., Jasaitis, A., Backgren, C., Puustinen, A., and Verkhovsky, M. I. (2000) The role of the D- and K-pathways of proton tranfer in the function of the haem-copper oxidases, *Biochim. Biophys. Acta 1459*, 514−520.
90. Brändén, M., Sigurdson, H., Namslauer, A., Gennis, R., Ädelroth, P., and Brzezinski, P. (2001) On the role of the K-proton-transfer pathway in cytochrome *c* oxidase, *Proc. Natl. Acad. Sci. U.S.A. 98*, 5013−5018.
91. Wikström, M., Verkhovsky, M. I., and Hummer, G. (2003) Water-gated mechanism of proton translocation by cytochrome *c* oxidase, *Biochim. Biophys. Acta 1604*, 61−65.
92. Michel, H. (1998) The mechanism of proton pumping by cytochrome *c* oxidase, *Proc. Natl. Acad. Sci. U.S.A. 95*, 12819−12824.
93. Rich, P. R. (2003) The molecular machinery of Keilin's respiratory chain, *Biochem. Soc. Trans. 31*, 1095−1105.
94. Babcock, G. T. (1999) How oxygen is activated and reduced in respiration, *Proc. Natl. Acad. Sci. U.S.A. 96*, 12971−12973.
95. Wikström, M. (2004) Cytochrome *c* oxidase: 25 years of the elusive proton pump, *Biochim. Biophys. Acta 1655*, 241−247.
96. Zaslavsky, D., and Gennis, R. (2000) Proton pumping by cytochrome oxidase: progress, problems and postulates, *Biochim. Biophys. Acta 1458*, 164−179.
97. Ayala, I., Rangel, K., York, D., and Barry, B. A. (2002) Spectroscopic properties of tyrosyl radicals in dipeptides, *J. Am. Chem. Soc. 124*, 5496−5505.
98. Cappuccio, J. A., Ayala, I., Elliot, G. I., Szundi, I., Lewis, J., Konopelski, J. P., Barry, B. A., and Einarsdóttir, Ó. (2002) Modeling the active site of cytochrome oxidase: synthesis and characterization of a cross-linked histidine-phenol, *J. Am. Chem. Soc. 124*, 1750−1760.
99. Aki, M., Ogura, T., Naruta, Y., Le, T. H., Sato, T., and Kitagawa, T. (2002) UV resonance Raman characterization of model compounds of $Tyr^{244}$ of bovine cytochrome *c* oxidase in its neutral, deprotonated anoionic, and deprotonated neutral radical forms: effects of covalent binding between tyrosine and histidine, *J. Phys. Chem. A 106*, 3436−3444.
100. McCauley, K. M., Vrtis, J. M., Dupont, J., and van der Donk, W. A. (2000) Insights into the functional role of the tyrosine-histidine linkage in cytochrome *c* oxidase, *J. Am. Chem. Soc. 122*, 2403−2404.
101. Pinakoulaki, E., Pfitzner, U., Ludwig, B., and Varotsis, C. (2002) The role of the cross-linked His-Tyr in the functional properties of the binuclear center in cytochrome *c* oxidase, *J. Biol. Chem. 277*, 13563−13568.
102. Tomson, F., Bailey, J. A., Gennis, R. B., Unkefer, C. J., Li, Z., Silks, L. A., Martinez, R. A., Donohoe, R. J., Dyer, R. B., and Woodruff, W. H. (2002) Direct infrared detection of the covalently ring linked His-Tyr structure in the active site of the heme-copper oxidases, *Biochemistry 41*, 14383−14390.
103. Berthomieu, C., and Hienerwadel, R. (2004) Vibrational spectroscopy to study the properties of redox-active tyrosines in photosystem II and other proteins, *Biochim. Biophys. Acta* (in press).
104. Hienerwadel, R., Boussac, A., Breton, J., and Berthomieu, C. (1997) Fourier transform infrared difference spectroscopy of photosystem II tyrosine D using site-directed mutagenesis and specific isotope labeling, *Biochemistry 36*, 14712−14723.
105. Buse, G., Soulimane, T., Dewor, M., Meyer, H. E., and Bluggel, M. (1999) Evidence for a copper-coordinated histidine-tyrosine cross-link in the active site of cytochrome oxidase, *Protein Sci. 8*, 985−990.

BI048545J